52nd IEEE Conference on Decision and Control
December 10-13, 2013. Florence, Italy

Profit Maximizing Storage Allocation in Power Grids

Anya Castillo and Dennice F. Gayme

Abstract— **This work investigates the interaction between nodal price signals and the optimal allocation and operation of distributed energy storage systems (ESS) in alternating current (AC) power networks. We model a multi-period optimal power flow (OPF) problem with charge and discharge dynamics for energy storage collocated with load and/or generation. We then apply a convex relaxation based on semidefinite programming (SDP) and derive the storage subproblem from the Lagrangian dual. We use the storage subproblem to investigate the relationship between the storage variables and the locational marginal prices (LMPs), which are market-based price signals defined by the dual variables associated with the nodal active power flow balance. Our theoretical results prove that LMPs drive charging and discharging dynamics, and that storage is allocated and operated to maximize the storage operator's profits, i.e. minimize the system costs in a purely competitive market. We then use this framework to illustrate LMP-based storage dynamics.**

I. INTRODUCTION

Energy storage systems (ESS) are becoming an attractive option in deregulated electricity markets. The increasing integration of variable renewable energy resources, such as wind and solar, requires complementary technologies such as energy storage to provide grid stability, online capacity, and fast-ramping energy services. The potential benefits of utility-scaled energy storage includes deferring investments in generation and transmission assets, providing fast-response ancillary services, improving load following, facilitating load shifting as well as improving power quality and service reliability [1].

There is a large body of work focusing ESS integration. References [2], [3], [4] and [5] indicate factors that drive energy storage investment. References [6] and [7] couple energy storage with wind farm operations to reduce forecasting errors and spinning reserve requirements. However these studies neglect the effects of losses and network congestion, which may lead to underestimation in the value of storage. Other studies incorporate operational and physical constraints through the optimal power flow (OPF) formulation, which is a nonconvex problem. Since the OPF is nonconvex and NP-hard, numerous studies solve an approximation; references [8], [9] and [10] solve a lossless approximation to assess optimal sizing and charge scheduling. This approach is problematic because actual power systems operate on alternating current (AC) networks, for which losses due to line resistances can be substantially lowered by raising the voltages [11].

Recently [12], [13], [14], [15] and [16] applied the full OPF to study ESS integration. Whereas [14] and [16] focus on the economic potential of preexisting storage, [12] investigate the allocation of energy storage to minimize curtailed wind energy. Reference [15] proposes a SDP relaxation of the OPF problem that includes simple storage dynamics, and the tandem study in [13] raises several questions regarding the role of network topology on storage placement. However by overlooking the effect of market-based price signals such as locational marginal prices (LMPs), the above studies lack a fundamental explanation of what drives the potential for grid-scale storage integration. The LMP is a price signal for resource investment and operations in competitive electricity markets, and consists of the marginal unit cost, congestion cost, and cost due to losses. In actual electricity markets, the LMPs are determined by either solving an OPF problem or solving an OPF approximation with losses, and then checking for feasibility in the full OPF problem [17].

In this study we derive the relation between LMPs and ESS allocation and operation. There are three main contributions of this paper. First we extend the OPF formulation with storage dynamics in [13] and [15] to include roundtrip efficiency of storage, thermal limits of lines, and ramp rates for conventional generators. We also account for charging and discharging dynamics separately, which enables a richer understanding of ESS allocation and operations. Second we derive a storage subproblem from the Lagrangian dual and present theory regarding the relationships between different modes of storage operation and LMPs. Third, we prove that storage is allocated and operated to maximize the storage operator's profits, i.e. minimize the system costs in a purely competitive market. The problem formulation and semidefinite program (SDP) solution method are described in Sections II and III. Theory on optimal storage dynamics is presented in Section IV. We investigate LMP-based storage dynamics with case studies for a modified IEEE 14-bus benchmark system in Section V, and conclude our work in Section VI.

II. PROBLEM FORMULATION

Consider a power network with the set of buses $\mathcal{N} := \{1, \ldots, N\}$, the set of generator buses $\mathcal{G} \subseteq \mathcal{N} := \{1, \ldots, G\}$, and the set of line flows $\mathcal{K} := \{1, \ldots, K\}$ where $k\,(n, i)$ is the flow on line k from bus n to bus i. Let $Y \in \mathbb{C}^{N \times N}$ denote the complex nodal admittance matrix and $Y^{\ell} \in \mathbb{C}^{K \times N}$ denote the complex branch admittance matrix, where the network elements are represented with equivalent

A. Castillo is with the Department of Geography and Environmental Engineering, Johns Hopkins University, Baltimore, MD 21218 USA anya.castillo@jhu.edu

D. Gayme is with the Department of Mechanical Engineering, Johns Hopkins University, Baltimore, MD 21218 USA dennice@jhu.edu

Π models, as defined in [18]. We assume balanced, three-phase, steady-state conditions and apply the conventional per-unit (p.u.) representation of all quantities. We model multi-period operations for power balancing in the real-time energy imbalance market for the discrete time intervals $t \in \mathcal{T} := \{1, \ldots, T\}$, where $\mathcal{T} \subset \tilde{\mathcal{T}}$ and $\tilde{\mathcal{T}} := \{0, \ldots, T\}$.

For the ESS capacity in each time interval t, the active power rates at each bus $n \in \mathcal{N}$ and time $t \in \mathcal{T}$ are bounded as

$$0 \leq r_n^c(t) \leq R_n^c \tag{1}$$

for the charging rate and

$$0 \leq r_n^d(t) \leq R_n^d \tag{2}$$

for the discharging rate. There are also corresponding reactive power capacity limits where $z_n(t)$ represents the inductive, i.e. $z_n(t) < 0$, or capacitive, i.e. $z_n(t) > 0$, ability of the ESS unit and is bounded as

$$Z_n^{min} \leq z_n(t) \leq Z_n^{max} \tag{3}$$

for every $n \in \mathcal{N}$, $t \in \mathcal{T}$. We define the energy storage level s_n of the ESS unit at each bus $n \in \mathcal{N}$ and time $t \in \mathcal{T}$ as

$$s_n(t) = s_n(t-1) + \eta^c r_n^c(t) - \left(\eta^d\right)^{-1} r_n^d(t) \tag{4}$$

where the respective charge and discharge efficiencies are denoted η^c and η^d. For a single operating cycle equivalent to the time horizon $\mathcal{T}$, we assume that the terminal storage levels of the prior operating cycle $t = 0 \in \tilde{\mathcal{T}}$ in the current operating cycle,

$$s_n(0) - s_n(T) = 0 \tag{5}$$

for all buses $n \in \mathcal{N}$. We limit the energy storage level $s_n(t)$ at all $n \in \mathcal{N}$, $t \in \mathcal{T}$ by

$$0 \leq s_n(t) \leq C_n \tag{6}$$

where C_n is the energy storage capacity at each bus $n \in \mathcal{N}$. The network energy storage capacity is limited by

$$\sum_{n \in \mathcal{N}} C_n \leq h. \tag{7}$$

At each bus $n \in \mathcal{N}$ and time $t \in \mathcal{T}$, the voltage magnitude $|V_n(t)|$ is bounded by

$$\left(V_n^{min}\right)^2 \leq |V_n(t)|^2 \leq \left(V_n^{max}\right)^2 \tag{8}$$

where $V_n(t) = V_n^r(t) + \mathbf{j} V_n^j(t)$ is the voltage phasor and $\mathbf{j} := \sqrt{-1}$. At all $n \in \mathcal{N}$, $t \in \mathcal{T}$ we denote the active and reactive power demands as $P_n^d(t)$ and $Q_n^d(t)$. At each bus $n \in \mathcal{G}$ and time $t \in \mathcal{T}$ the active and reactive power generation, $P_n^g(t)$ and $Q_n^g(t)$, are bounded by the capacity constraints

$$P_n^{min} \leq P_n^g(t) \leq P_n^{max} \tag{9}$$

$$Q_n^{min} \leq Q_n^g(t) \leq Q_n^{max} \tag{10}$$

respectively. Assuming arbitrary active power generation at $t = 1$, the active power ramp rates on conventional generators for time $t \in \{2, \ldots, T\}$ at each bus $n \in \mathcal{G}$ are

$$-RR_n \leq P_n^g(t) - P_n^g(t-1) \leq RR_n. \tag{11}$$

Furthermore, the apparent power flow for every $t \in \mathcal{T}$ on each line $k \in \mathcal{K}$ from bus n to bus i is limited as follows:

$$\left(P_{k(n,i)}^{\ell}(t)\right)^2 + \left(Q_{k(n,i)}^{\ell}(t)\right)^2 \leq (S_k^{max})^2 \tag{12}$$

where $P_{k(n,i)}^{\ell}(t)$ and $Q_{k(n,i)}^{\ell}(t)$ are determined based on the system branch admittance matrix Y^{ℓ}.

We denote $I_n(t)$ as the current phasor at bus $n \in \mathcal{N}$ for time $t \in \mathcal{T}$, where the current vector $\mathbf{I}(t) := [I_1(t) \cdots I_N(t)]^T$ is defined as $\mathbf{I}(t) = Y\mathbf{V}(t)$ for the admittance matrix Y and the voltage vector $\mathbf{V}(t) := [V_1(t) \cdots V_N(t)]^T$. By Kirchhoff's laws, $V_n(t)[I_n(t)]^* = P_n(t) + \mathbf{j} Q_n(t)$ balances the power for each bus $n \in \mathcal{N}$ and time $t \in \mathcal{T}$ where $(\cdot)^*$ denotes the complex conjugate. Therefore the active power injection is

$$P_n(t) = P_n^g(t) - P_n^d(t) - \left(r_n^c(t) - r_n^d(t)\right) \tag{13}$$

and the reactive power injection is

$$Q_n(t) = Q_n^g(t) - Q_n^d(t) - z_n(t). \tag{14}$$

Let $\mathbf{V}$, $\mathbf{r}^c$, $\mathbf{r}^d$, $\mathbf{z}$, $\mathbf{P}^g$, $\mathbf{Q}^g$, $\mathbf{P}^{\ell}$, $\mathbf{Q}^{\ell}$, and $\mathbf{C}$ respectively denote the following decision variables $\{V_n(t)\}_{\mathcal{N}\times\mathcal{T}}$, $\{r_n^c(t)\}_{\mathcal{N}\times\mathcal{T}}$, $\{r_n^d(t)\}_{\mathcal{N}\times\mathcal{T}}$, $\{z_n(t)\}_{\mathcal{N}\times\mathcal{T}}$, $\{P_n^g(t)\}_{\mathcal{G}\times\mathcal{T}}$, $\{Q_n^g(t)\}_{\mathcal{G}\times\mathcal{T}}$, $\{P_k^{\ell}(t)\}_{\mathcal{K}\times\mathcal{T}}$, $\{Q_k^{\ell}(t)\}_{\mathcal{K}\times\mathcal{T}}$ and $\{C_n\}_{\mathcal{N}\times\mathcal{T}}$. Let $\mathbf{s}$ denote the set $\{s_n(t)\}_{\mathcal{N}\times\tilde{\mathcal{T}}}$. In combining the above expressions we formulate the following multi-period, nonlinear OPF with storage dynamics, which we refer to as OPF+S:

$$\mathbf{p^{opt}} := \min_{\mathbf{V},\mathbf{r}^c,\mathbf{r}^d,\mathbf{z},\mathbf{P}^g,\mathbf{Q}^g,\mathbf{P}^{\ell},\mathbf{Q}^{\ell},\mathbf{C}} \; f(\cdot, t) \tag{15}$$

subject to

$$(1) - (14) \tag{16}$$

where

$$f(\cdot, t) = \sum_{t \in \mathcal{T}} \left\{ \sum_{n \in \mathcal{G}} f_n^g\left(P_n^g(t), t\right) + \sum_{n \in \mathcal{N}} f_n^s\left(r_n^d(t), t\right) \right\} \tag{17}$$

The multi-period cost function in (17) denotes the cost of generating active power and discharging storage. We assume negligible marginal cost for renewable resources, and strictly convex quadratic cost functions for both conventional generators, i.e. $f_n^g\left(P_n^g(t), t\right) = c_{n2}^g(t)\left(P_n^g(t)\right)^2 + c_{n1}^g(t) P_n^g(t)$, and ESS units, i.e. $f_n^s\left(r_n^d(t), t\right) = c_{n2}^s(t)\left(r_n^d(t)\right)^2 + c_{n1}^s(t) r_n^d(t)$. The cost of charging is not included in f_n^s because implicitly the storage operator pays the LMP.

III. SOLUTION TECHNIQUE

The lower bound on the voltage magnitude in (8) and the power balance in (13) and (14) are nonconvex quadratic constraints. Therefore nonlinear programming methods are not guaranteed to find a solution that is *globally* optimal. Based on the semidefinite relaxations in [19] and [20], we apply an approximate but convex reformulation of the OPF+S problem formulation (15) and (16) in III-A and III-B.

A. Primal Relaxation

We define $W(t) := \omega(t)\omega(t)^T \in \mathbb{R}^{2N\times 2N}$ for all $t \in \mathcal{T}$ where $\omega(t) = \left[V^r(t)^T \quad V^j(t)^T\right]^T$. We also define $\overline{Y}_n := e_n e_n^T Y$ for each bus $n \in \mathcal{N}$ and $\overline{Y}^{\ell}_{k(n,i)} := (y^s_n + y_{ni}) e_n e_n^T - (y_{ni}) e_n e_i^T$ for each line $k \in \mathcal{K}$, where y^s_n is the shunt component of the admittance term y_n, $e_n \in \mathbb{R}^N$ is the standard basis vector, and $\mathrm{Re}\{\cdot\}$ and $\mathrm{Im}\{\cdot\}$ denote the real and imaginary parts of their arguments, respectively. We then define $\Phi_n := h\left(\overline{Y}_n\right)$ for $h : \mathbb{C}^{N\times N} \to \mathbb{R}^{2N\times 2N}$ and $\Phi^{\ell}_k := h\left(\overline{Y}^{\ell}_k\right)$ for $h : \mathbb{C}^{K\times N} \to \mathbb{R}^{2N\times 2N}$ where

$$h(\Omega) := \frac{1}{2}\begin{bmatrix} \mathrm{Re}\{\Omega + \Omega^T\} & \mathrm{Im}\{\Omega - \Omega^T\} \\ \mathrm{Im}\{\Omega - \Omega^T\} & \mathrm{Re}\{\Omega + \Omega^T\} \end{bmatrix}.$$

Similarly we define $\Psi_n := \tilde{h}\left(\overline{Y}_n\right)$ for $\tilde{h} : \mathbb{C}^{N\times N} \to \mathbb{R}^{2N\times 2N}$ and $\Psi^{\ell}_k := \tilde{h}\left(\overline{Y}^{\ell}_k\right)$ for $\tilde{h} : \mathbb{C}^{K\times N} \to \mathbb{R}^{2N\times 2N}$ where

$$\tilde{h}(\Omega) := -\frac{1}{2}\begin{bmatrix} \mathrm{Im}\{\Omega + \Omega^T\} & \mathrm{Re}\{\Omega^T - \Omega\} \\ \mathrm{Re}\{\Omega^T - \Omega\} & \mathrm{Im}\{\Omega + \Omega^T\} \end{bmatrix}.$$

The active and reactive power injections for each bus $n \in \mathcal{N}$ can be expressed as $\mathrm{tr}\{\Phi_n W(t)\}$ and $\mathrm{tr}\{\Psi_n W(t)\}$ where $\mathrm{tr}\{\cdot\}$ is the trace operator; similarly, the active and reactive power flows on each line $k \in \mathcal{K}$ can be expressed as $\mathrm{tr}\left\{\Phi^{\ell}_k W(t)\right\}$ and $\mathrm{tr}\left\{\Psi^{\ell}_k W(t)\right\}$, respectively. We also define the coefficient matrix $M_n := e_n e_n^T \bigoplus e_n e_n^T$ to express the nodal voltages in a similar manner as $\mathrm{tr}\{M_n W(t)\}$ for each bus $n \in \mathcal{N}$.

Let $\mathbf{W}$, $\boldsymbol{\alpha}^{\boldsymbol{g}}$, $\boldsymbol{\alpha}^{\boldsymbol{s}}$ denote the decision variable sets $\{W(t)\}_{t\in\mathcal{T}}, \{\alpha^g_n(t)\}_{\mathcal{G}\times\mathcal{T}}$ and $\{\alpha^s_n(t)\}_{\mathcal{N}\times\mathcal{T}}$. We refer to the relaxation of OPF+S in (15) and (16) as the SDP-OPF+S:

$$\hat{\mathbf{p}}^{\mathbf{opt}} := \min_{\mathbf{W},\boldsymbol{\alpha}^{\boldsymbol{g}},\boldsymbol{\alpha}^{\boldsymbol{s}},\mathbf{r}^c,\mathbf{r}^d,\mathbf{z},\mathbf{P}^g,\mathbf{Q}^g,\mathbf{C}} \sum_{t\in\mathcal{T}}\sum_{n\in\mathcal{N}} \alpha^g_n(t) + \alpha^s_n(t) \tag{18}$$

subject to

$$\mathrm{tr}\{\Phi_n W(t)\} = P^g_n(t) - P^d_n(t) - \left(r^c_n(t) - r^d_n(t)\right) \tag{19a}$$
$$\mathrm{tr}\{\Psi_n W(t)\} = Q^g_n(t) - Q^d_n(t) - z_n(t) \tag{19b}$$
$$\left(V^{min}_n\right)^2 \le \mathrm{tr}\{M_n W(t)\} \le \left(V^{max}_n\right)^2 \tag{19c}$$
$$\begin{bmatrix} c^g_{n1}(t) P^g_n(t) - \alpha^g_n(t) & \sqrt{c^g_{n2}(t)} P^g_n(t) \\ \sqrt{c^g_{n2}(t)} P^g_n(t) & -1 \end{bmatrix} \preceq 0 \tag{19d}$$
$$\begin{bmatrix} c^s_{n1}(t) r^d_n(t) - \alpha^s_n(t) & \sqrt{c^s_{n2}(t)} r^d_n(t) \\ \sqrt{c^s_{n2}(t)} r^d_n(t) & -1 \end{bmatrix} \preceq 0 \tag{19e}$$
$$\begin{bmatrix} -\left(S^{max}_k\right)^2 & \mathrm{tr}\{\Phi^{\ell}_k W(t)\} & \mathrm{tr}\{\Psi^{\ell}_k W(t)\} \\ \mathrm{tr}\{\Phi^{\ell}_k W(t)\} & -1 & 0 \\ \mathrm{tr}\{\Psi^{\ell}_k W(t)\} & 0 & -1 \end{bmatrix} \preceq 0 \tag{19f}$$
$$W(t) \succeq 0 \tag{19g}$$
$$(1) - (7) \tag{19h}$$
$$(9) - (11) \tag{19i}$$

with $n \in \mathcal{N}$, $k \in \mathcal{K}$, and $t \in \mathcal{T}$. For the reformulated constraints, equations (19a)-(19e) apply to each bus $n \in \mathcal{N}$ and time $t \in \mathcal{T}$; equation (19f) applies to each line $k \in \mathcal{K}$ and time $t \in \mathcal{T}$; equation (19g) applies to all $t \in \mathcal{T}$. Note that SDP-OPF+S has a linear cost function (18), linear equality and inequality constraints in equations (19a)-(19c), and linear matrix inequality (LMI) constraints in (19d)-(19g).

The change of variables that transforms (15) and (16) into (18) and (19) follows from the fact that a symmetric matrix $W(t) \in \mathbb{R}^{2N\times 2N}$ is positive semidefinite and rank one if and only if there exists $\omega(t) \in \mathbb{R}^{2N}$ such that $W(t) = \omega(t)\omega(t)^T$ for all $t \in \mathcal{T}$. This condition can be enforced by including the following constraint in SDP-OPF+S:

$$\mathrm{rank}(W(t)) = 1 \tag{20}$$

for all $t \in \mathcal{T}$. However equation (20) is a nonconvex constraint, and therefore we can exclude (20) by analytically determining if the solution to SDP-OPF+S in (18) and (19) meets the rank one criteria. In the case when $\mathbf{W^{opt}}$ has a rank one solution, $\hat{\mathbf{p}}^{\mathbf{opt}}$ is the global optimum of the OPF+S problem and SDP-OPF+S is equivalent to OPF+S where $\hat{\mathbf{p}}^{\mathbf{opt}} = \mathbf{p}^{\mathbf{opt}}$, i.e. the SDP relaxation is exact. We now present the Lagrangian dual, which will be decomposed into the storage subproblem in Section IV.

B. Lagrangian Dual

The Lagrangian dual for the optimization problem (18) and (19) is

$$\hat{\mathbf{d}}^{\mathbf{opt}} := \max_{\boldsymbol{x}\ge 0,\boldsymbol{\lambda},\boldsymbol{\varphi},\boldsymbol{\xi},\boldsymbol{\nu},\boldsymbol{\varsigma},\boldsymbol{\zeta}} g(\cdot) \tag{21}$$

subject to

$$\sum_{n\in\mathcal{N}} \left\{\lambda_n(t)\Phi_n + \left(\theta^{max}_n(t) - \theta^{min}_n(t)\right) M_n + \varphi_n(t)\Psi_n\right\} + \sum_{k\in\mathcal{K}} \left\{2\mu^{(2)}_k(t)\Phi_k + 2\mu^{(3)}_k(t)\Psi_k\right\} \succeq 0 \tag{22a}$$
$$\rho^{max}_n(t) - \rho^{min}_n(t) + \lambda_n(t) - \xi_n(t)\eta^c = 0 \tag{22b}$$
$$\sigma^{max}_n(t) - \sigma^{min}_n(t) - \lambda_n(t) - \xi_n(t)\left(\eta^d\right)^{-1} + c^s_{n1}(t) + 2\sqrt{c^s_{n2}(t)}\varsigma_{n1}(t) = 0 \tag{22c}$$
$$\lambda^{max}_n(t) - \lambda^{min}_n(t) - \lambda_n(t) + \delta^{max}_n(t) - \delta^{min}_n(t) - \delta^{max}_n(t-1) + \delta^{min}_n(t-1) + c^g_{n1}(t) + 2\sqrt{c^g_{n2}(t)}\nu_{n1}(t) = 0 \tag{22d}$$
$$\varphi^{max}_n(t) - \varphi^{min}_n(t) - \varphi_n(t) = 0 \tag{22e}$$
$$\psi^{max}_n(t) - \psi^{min}_n(t) - \varphi_n(t) = 0 \tag{22f}$$
$$\xi_n(t) - \xi_n(t-1) + \beta^{max}_n(t) - \beta^{min}_n(t) = 0 \tag{22g}$$
$$\varrho - \beta^{max}_n(t) = 0 \tag{22h}$$
$$\nu_n(t) := \begin{bmatrix} 1 & \nu_{n1}(t) \\ \nu_{n1}(t) & \nu_{n2}(t) \end{bmatrix} \succeq 0 \tag{22i}$$
$$\varsigma_n(t) := \begin{bmatrix} 1 & \varsigma_{n1}(t) \\ \varsigma_{n1}(t) & \varsigma_{n2}(t) \end{bmatrix} \succeq 0 \tag{22j}$$
$$\zeta_k(t) := \begin{bmatrix} \zeta_{k1}(t) & \zeta_{k2}(t) & \zeta_{k3}(t) \\ \zeta_{k2}(t) & \zeta_{k4}(t) & \zeta_{k5}(t) \\ \zeta_{k3}(t) & \zeta_{k5}(t) & \zeta_{k6}(t) \end{bmatrix} \succeq 0 \tag{22k}$$

where the cost function in (21) is

$$
\begin{aligned}
& g(\cdot) := \\
& -\varrho h - \sum_{t=2}^{T} \sum_{n \in \mathcal{N}} RR_n \left(\delta_n^{min}(t) + \delta_n^{max}(t) \right) \\
& + \sum_{t \in \mathcal{T}} \sum_{n \in \mathcal{N}} \Big\{ \lambda_n(t) P_n^d(t) + \varphi_n(t) Q_n^d(t) + c_{n1}^s(t) \\
& + 2\sqrt{c_{n2}^s(t)}\varsigma_{n1}(t) - \varsigma_{n2}(t) + \lambda_n^{min}(t) P_n^{min} \\
& - \lambda_n^{max}(t) P_n^{max} + \varphi_n^{min}(t) Q_n^{min} - \varphi_n^{max}(t) Q_n^{max} \\
& + \vartheta_n^{min}(t) \left(V_n^{min}\right)^2 - \vartheta_n^{max}(t) (V_n^{max})^2 - \rho_n^{max}(t) R^c \\
& - \sigma_n^{max}(t) R^d + \psi_n^{min}(t) Z^{min} - \psi_n^{max}(t) Z^{max} \Big\} \\
& + \sum_{t \in \mathcal{T}} \sum_{n \in \mathcal{G}} \left(c_{n1}^g(t) + 2\sqrt{c_{n2}^g(t)}\nu_{n1}(t) - \nu_{n2}(t) \right) \\
& + \sum_{t \in \mathcal{T}} \sum_{k \in \mathcal{K}} \left(\zeta_{k1}(t) (S_k^{max})^2 + \zeta_{k4}(t) + \zeta_{k6}(t) \right)
\end{aligned} \tag{23}
$$

with $n \in \mathcal{N}$, $k \in \mathcal{K}$, and $t \in \mathcal{T}$. For equation (22d), $\delta_n^{min}(t-1) = 0$ and $\delta_n^{max}(t-1) = 0$ terms when $t = 1$. For equation (22g), $\xi_n(0)$ and $\xi_n(T)$ are sign indefinite.

Accordingly, let $\boldsymbol{\lambda}$, $\boldsymbol{\varphi}$, and $\boldsymbol{\xi}$ denote the respective sign indefinite dual variable sets $\{\lambda_n(t)\}_{\mathcal{N}\times\mathcal{T}}$, $\{\varphi_n(t)\}_{\mathcal{N}\times\mathcal{T}}$, and $\{\xi_n(t)\}_{\mathcal{N}\times\tilde{\mathcal{T}}}$. Also let $\boldsymbol{\nu}, \boldsymbol{\varsigma}$ and $\boldsymbol{\zeta}$ denote the respective Lagrange multiplier matrix sets $\{\nu_n(t)\}_{\mathcal{G}\times\mathcal{T}}$, $\{\varsigma_n(t)\}_{\mathcal{N}\times\mathcal{T}}$, and $\{\zeta_k(t)\}_{\mathcal{K}\times\mathcal{T}}$ that are associated with the LMI constraints in (19d), (19e) and (19f), respectively. Finally, let $\boldsymbol{x}$ denote the set of remaining nonnegative decision variable sets.

Therefore we define the Lagrangian dual problem D-SDP-OPF+S, which is a convex problem, by equations (21) and (22). By solving for $\hat{\mathbf{d}}^{\mathbf{opt}}$, we can determine the best (largest) lower bound for all the primal variables in SDP-OPF+S. Moreover since the primal problem SDP-OPF+S is also convex, the KKT conditions are sufficient for the solution to be both primal and dual optimal. Gayme and Topcu [15] prove that, excluding the rank constraint, strong duality holds by Slater's condition.

IV. OPTIMAL STORAGE DYNAMICS

In this section we derive the storage subproblem in IV-A and associate the LMP with ESS allocation and operations. We then present conditions in IV-B and IV-C to avoid such simultaneous charging and discharging. We also provide insight on storage operations in IV-C, and finally we prove our main result on ESS allocation and operations in IV-D.

Within the OPF framework, the LMP at each bus n is the dual variable λ_n associated with the active power balance in (13) and accounts for the marginal unit cost, congestion cost, and cost due to losses. The LMP at bus n depends on both the time of operations and the location of bus n within the network. Since active power injections $P_n^g(t)$ and $r_n^d(t)$ are the decision variables in the objective function (17), the dual variable associated with constraint (13) indicates the value of dispatching an additional unit of active power at bus n.

A. Storage Subproblem

We decompose D-SDP-OPF+S in (21) and (22) in order to gain intuition on optimal storage allocation and operations in the SDP-OPF+S problem. Thus, we extract the primal variables related to the ESS units on the network, i.e. the active power charge rate $\mathbf{r^c}$, the active power discharge rate $\mathbf{r^d}$, the reactive power capability $\mathbf{z}$, the storage level $\mathbf{s}$, and the storage capacity $\mathbf{C}$. This decomposition leads to the following subproblem:

$$
g_s(\boldsymbol{\lambda}, \boldsymbol{\varphi}) = \min_{\mathbf{r^c}, \mathbf{r^d}, \mathbf{z}, \mathbf{C}} \ \Lambda_s \tag{24}
$$

subject to

$$
\text{(19h)} \tag{25}
$$

The corresponding Lagrangian is

$$
\begin{aligned}
\Lambda_s = & f_n^s\left(r_n^d(t), t\right) + \\
& \sum_{t \in \mathcal{T}} \sum_{n \in \mathcal{N}} \Big\{ \lambda_n(t) \left[r_n^c(t) - r_n^d(t) \right] + \varphi_n(t) \left[z_n(t) \right] \Big\}.
\end{aligned} \tag{26}
$$

Since active power is priced and reactive power is not priced in the real-time energy imbalance markets, $\lambda_n(t) \gg \varphi_n(t)$ for all $t \in \mathcal{T}$. This fact has strong implications for our main result in IV-D.

B. Guaranteeing Positive LMPs for Storage Optimization

Negative LMPs are common in the power markets and may result from negative offer curves or binding line flow constraints, as a couple of examples. However the SDP relaxation is not guaranteed to yield a zero duality gap under these conditions [20]. A negative LMP implies that an ESS unit would be paid to charge and pay to discharge during the same time step, and therefore can result in multimodal operations such as simultaneous charging and discharging or instantaneous cycling of 'realistic' ESS units, i.e. where the ESS roundtrip efficiency is less than 100%, to dissipate enough excess energy on the power grid. This fact leads us to the following lemma:

Lemma 1: $\lambda_n(t) \geq 0$ for $\forall n \in \mathcal{N}, t \in \mathcal{T}$ if and only if $P_n(t) + P_n^d(t) + r_n^c(t) \leq P_n^g(t) + r_n^d(t)$.

Proof. ($\Longleftarrow$) The active power balance constraint in (19a) can be rewritten as the following two inequalities

$$
P_n(t) + P_n^d(t) + r_n^c(t) \leq P_n^g(t) + r_n^d(t), \ \lambda_n^+(t) \tag{27a}
$$

$$
P_n(t) + P_n^d(t) + r_n^c(t) \geq P_n^g(t) + r_n^d(t), \ \lambda_n^-(t) \tag{27b}
$$

for all $t \in \mathcal{T}$, $n \in \mathcal{N}$ where $\lambda_n^+(t), \lambda_n^-(t) \geq 0$. The $\lambda_n(t)$ terms of the dual problem in (21) and (22) can be replaced by $(\lambda_n^+(t) - \lambda_n^-(t))$ where

$$
\lambda_n^+(t) - \lambda_n^-(t) \geq 0. \tag{28}
$$

This implies that if $\lambda_n^+(t) \geq \lambda_n^-(t)$, then $P_n(t) + P_n^d(t) + r_n^c(t) \leq P_n^g(t) + r_n^d(t)$.

($\Longrightarrow$) Assuming we replace the equality constraint in (19a) by the inequality

$$
P_n(t) + P_n^d(t) + r_n^c(t) \leq P_n^g(t) + r_n^d(t), \tag{29}
$$

and suppose $\hat{P}_n^g(t)$, $\hat{r}_n^c(t)$, $\hat{r}_n^d(t)$, and $\hat{P}_n(t) = \mathrm{tr}\left\{\Phi_n \hat{W}(t)\right\}$ for all $n \in \mathcal{N}, t \in \mathcal{T}$ is a feasible solution to the problem in (18), (19b)-(19i) and (29). By dual feasibility, the dual problem $\hat{\mathbf{d}}^{\mathbf{opt}}$ gives a nontrivial lower bound on

$\hat{\mathbf{p}}^{\mathbf{opt}}$ only when (29) is binding, which implies $\lambda_n(t) \geq 0$ for all $n \in \mathcal{N}, t \in \mathcal{T}$. ■

Therefore we can guarantee nonnegative dual variables for the storage optimization problem by enforcing the inequality constraint in (29) for the active power balance, and then checking the solution to determine whether there was an over-supply of power for any time t. Furthermore, we have $\lambda > 0$ only when constraint (29) is binding, which will become useful in simulating the charge and discharge behavior as we prove below.

C. Unimodal Storage Dynamics

Multimodal operations in storage dynamics are not valuable when LMPs are positive, as we prove below.

Theorem 1: For energy storage capacity at bus $n \in \mathcal{N}$ where $C_n > 0$, if $\lambda_n(t)$ is strictly positive then $r_n^c(t)$ and $r_n^d(t)$ are never simultaneously nonzero, i.e. simultaneous charging and discharging will not occur.

Proof. For the storage subproblem in (24) and (25), include the constraints (1) and (2) on the active power charge and discharge rates into the Lagrangian of (26). The KKT conditions of this modified storage subproblem consist of the constraints $(3)-(7)$, the following complementary slackness conditions

$$\varphi_n(t)\left[z_n(t)\right] = 0, \tag{30a}$$
$$\lambda_n(t)\left[r_n^c(t) - r_n^d(t)\right] = 0, \tag{30b}$$
$$\left[\rho_n^{max}(t) - \rho_n^{min}(t)\right] r_n^c(t) = 0, \tag{30c}$$
$$\left[\sigma_n^{max}(t) - \sigma_n^{min}(t)\right] r_n^d(t) = 0, \tag{30d}$$

and the zero gradient condition on $\mathbf{r^c}$ and $\mathbf{r^d}$

$$\begin{aligned}\begin{bmatrix} \nabla_{r^c}\Lambda_s \\ \nabla_{r^d}\Lambda_s \end{bmatrix} := \quad & \begin{bmatrix} \nabla_{r^c} f \\ \nabla_{r^d} f \end{bmatrix} + \begin{bmatrix} 1 \\ -1 \end{bmatrix} \lambda_n(t) \\ & + \begin{bmatrix} 1 \\ 0 \end{bmatrix} \left(\rho_n^{max}(t) - \rho_n^{min}(t)\right) \\ & + \begin{bmatrix} 0 \\ 1 \end{bmatrix} \left(\sigma_n^{max}(t) - \sigma_n^{min}(t)\right) = 0\end{aligned} \tag{31}$$

for all $n \in \mathcal{N}$ and $t \in \mathcal{T}$. The Lagrange multipliers $\boldsymbol{\lambda}$ and $\boldsymbol{\varphi}$ are sign indefinite, and $\boldsymbol{\rho}, \boldsymbol{\sigma} \geq 0$. From (26) we have that $\nabla_{r^c} f = 0$ and for strictly positive $\lambda_n(t)$

$$\begin{aligned} -\nabla_{r^d} f + & \left(\rho_n^{min}(t) - \rho_n^{max}(t)\right) \\ & + \left(\sigma_n^{min}(t) - \sigma_n^{max}(t)\right) > 0. \end{aligned} \tag{32}$$

Assuming f is strictly convex, we have $\nabla_{r^d} f > 0$, which implies $-\nabla_{r^d} f < 0$ and therefore $\rho_n^{max}(t)$ and $\sigma_n^{max}(t)$ can never both be positive simultaneously. When either but not both $\rho_n^{min}(t)$ or $\sigma_n^{min}(t)$ are nonzero, the storage device is exclusively charging or discharging, respectively. In the event that both $\rho_n^{min}(t)$ and $\sigma_n^{min}(t)$ are nonzero, then the storage device is neither charging nor discharging. ■

Remark 1: To assume $\nabla_{r^d} f > 0$ for the cost function given in equation (17), we must ensure that

$$2c_{n2}^s(t)\, r_n^d(t) + c_{n1}^s(t) > 0. \tag{33}$$

Therefore we can assume that the storage is not simultaneously charging and discharging as long as $\lambda_n(t) > 0$ or there is an over-supply (see Lemma 1).

D. Profit Maximizing Storage Dynamics

The LMP elicits varying storage dynamics depending upon the magnitude of the dual variables and whether the dual variables λ are positive or negative. Here we use the storage subproblem in (24) and (25) to prove that in a perfectly competitive market, the storage profits are maximized when the total system costs are minimized.

Theorem 2: For an arbitrary operating cycle $\mathcal{T} := \{1, \ldots, T\}$, the energy storage capacity C_n receives the most incremental value at the bus n where

$$\max_n \left(\max_{\boldsymbol{\lambda}, \boldsymbol{\varphi}} \ \pi_n^{s,\mathrm{opt}} \right) \tag{34}$$

for

$$\begin{aligned} \pi_n^{s,\mathrm{opt}} \quad & = -f_n^s\left(r_n^d(t)^{\mathrm{opt}}, t\right) \\ & + \sum_{t \in \mathcal{T}} \Big(\lambda_n(t)^{\mathrm{opt}} \left[r_n^d(t)^{\mathrm{opt}} - r_n^c(t)^{\mathrm{opt}} \right] \\ & - \varphi_n(t)^{\mathrm{opt}} \left[z_n(t)^{\mathrm{opt}} \right] \Big). \end{aligned} \tag{35}$$

Proof. From the subproblem in (24) we have

$$\hat{\mathbf{d}}_{\mathbf{s}}^{\mathbf{opt}} := \max_{\boldsymbol{\lambda}, \boldsymbol{\varphi}} \ g_s(\boldsymbol{\lambda}, \boldsymbol{\varphi}) \tag{36}$$

where $g_s(\boldsymbol{\lambda}, \boldsymbol{\varphi})$ is equivalent to

$$\hat{g}_s(\boldsymbol{\lambda}, \boldsymbol{\varphi}) = \max_{\mathbf{r^c}, \mathbf{r^d}, \mathbf{z}, \mathbf{C}} \ \sum_{n \in \mathcal{N}} \pi_n^s. \tag{37}$$

For $C_n > 0$ in the optimal solution $\hat{\mathbf{p}}^{\mathbf{opt}}$, the profit to C_n must be nonnegative, i.e. $\pi_n^s \geq 0$. Moreover, the most profits are attained at bus n where (34) holds. ■

Corollary 1: For the overall network we have

$$\boldsymbol{\pi}^{\boldsymbol{s,\mathrm{opt}}} = \max_{\boldsymbol{\lambda}, \boldsymbol{\varphi}} \ \hat{g}_s(\boldsymbol{\lambda}, \boldsymbol{\varphi}) \geq 0 \tag{38}$$

which drives optimal storage allocation and operation. The optimization $\boldsymbol{\pi}^{\boldsymbol{s,\mathrm{opt}}}$ in (38) holds true for the optimal solution $\hat{\mathbf{d}}^{\mathbf{opt}}$ in (21) and (22), which minimizes the total system costs in (18) and (19) for a perfectly competitive market.

V. CASE STUDIES

In this section we demonstrate LMP-based storage dynamics using the topology of the 14-bus IEEE benchmark system [21] in Fig. 1 using the solution procedure for SDP-OPF+S discussed in Section III-A. The demand profiles for each bus, shown in Fig. 2, are based on data from Southern California Edison for July 2010 and are measured at half-hour intervals [13]. We apply time-invariant quadratic cost functions for the generators [22]. We define the above case as our baseline scenario. Unless otherwise indicated, all power values are normalized to per unit (p.u.) for a base of 100 MVA, as described in [18].

We consider a single grid-scale energy storage technology with charging and discharging power rates of 8MW per

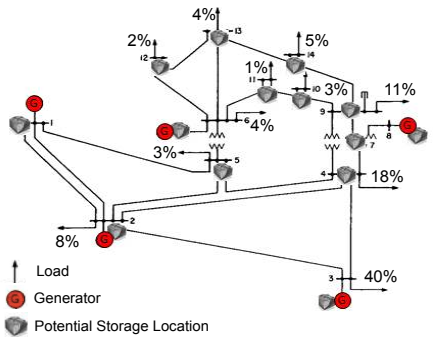

Fig. 1: The topology of the 14-bus IEEE benchmark system with the overall demand percentage for the operating cycle reported at each bus; note bus 3 has the highest net demand, which is equal to 40% of the overall network demand, followed by bus 4 and then bus 9.

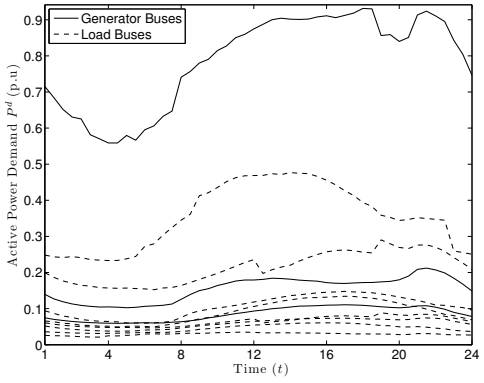

Fig. 2: Active power demand profiles for each of the 14 buses based on actual feeder data for an average day in Southern California, July 2010.

half-hour time interval (i.e. $R_c = R_d = 0.08$ p.u. for a power base 100 MVA), a roundtrip efficiency of 81% (i.e. $\eta_n^c = \eta_n^d = 0.9$), and no VAr support (i.e. $Z^{max} = Z^{min} = 0$). The operational cost of charging is the LMP at the bus and the operational cost of discharging is set to an infinitesimal quantity (i.e. $c_{n2}^s(t) = 10^{-3}$) to prevent simultaneous charging and discharging (see Remark 1 for Theorem 1 in Section IV-C). We solve SDP-OPF+S in (18) and (19), assuming that the energy storage capacity can be placed and operated at any bus n within the network, where the aggregated storage capacity is limited to $h = 1$ p.u. (i.e. 100 MWΔt).

We consider three scenarios, the baseline scenario which is defined above, a congested network scenario ($S_{(1,2)}^{max} = 0.8$, $S_{(1,5)}^{max} = 0.4$, $S_{(2,3)}^{max} = 0.3$, and $S_{(2,4)}^{max} = 0.3$ in p.u.), and finally a scenario where we double the line resistances $\mathcal{R}$ in the baseline scenario. Table I indicates that ESS is increasingly allocated to buses where there is the most potential for profits. The load-weighted average LMPs, i.e. $\overline{\lambda_n} = \left[\sum_{t\in\mathcal{T}} P_n^d(t)\cdot\lambda_n(t)\right] / \left[\sum_{t\in\mathcal{T}} P_n^d(t)\right]$, provide some indication of profitable storage allocations due to

TABLE I: Energy storage capacity C_n (in MWΔt), profits π_n^s (in \$K) and load-weighted average LMP $\overline{\lambda_n^s}$ (in \$/MWΔt) at each bus n for the baseline case, the congested network, and the network with double the line resistances ($\mathcal{R}$); the average LMP is used for zero demand buses.

	Baseline Case			Congested Network			Doubled $\mathcal{R}$		
Bus	C_n	π_n^s	$\overline{\lambda_n}$	C_n	π_n^s	$\overline{\lambda_n}$	C_n	π_n^s	$\overline{\lambda_n}$
1	0	0	34.2	0	0	29.9	0	0	33.2
2	0	0	36.3	0	0	31.2	0	0	36
3	35.6	20.1	38.5	0	0	41	0.1	0	39.7
4	1.7	0.9	38	11.9	7.5	39.1	18.3	7	38.9
5	0	0	37.5	9.6	6.1	37.8	0.1	0	38.1
6	0	0	37.5	0.1	0.1	38.1	0.1	0	38.1
7	0.4	0.2	37.4	0.1	0	38.2	0.3	0.1	38.4
8	0.4	0.2	37.4	0.1	0	38.2	0.3	0.1	38.4
9	0.2	0.1	37.9	0	0	38.6	0.2	0.1	38.8
10	4.5	2.5	38	0.1	0.1	38.7	7.4	2.8	39
11	0	0	37.6	0.2	0.1	38.2	0.6	0.2	38.5
12	3.2	1.8	38.1	10.2	6.5	38.6	8	3.1	39.1
13	16.1	9.1	38.6	31.7	20	39.1	26.7	10.2	39.6
14	37.9	21.4	39.1	36	22.8	39.5	37.9	14.6	40.5
Total	100	56.3	N/A	100	63.2	N/A	100	38.2	N/A

network effects, but do not account for storage operations due to substantial or prolonged off-peak to peak price differences. For a lossless (i.e. all line resistances are zero) uncongested network, the energy storage capacity is allocated uniformly throughout the network because the LMP is determined purely by the marginal unit cost. In the baseline scenario, a large portion of the storage is allocated to accommodate the high demand at bus 3. Moreover, although buses 13 and 14 have relatively marginal demand in the network, ESS allocation to these buses is robust to both network congestion and increasing network resistance. Fig. 3a and 3b indicate aggregate storage dynamics over the operating cycle and the change in LMP due to ESS integration, respectively. According to Fig. 3a, network congestion causes higher off-peak generation in order to alleviate peak congestion. In the case of doubled network resistances, there is an overall increase in storage utilization in order to satisfy the higher active power losses on the network. Fig. 3b indicates that the LMPs can increase substantially during off-peak times, with slight decreases during the peak period. As illustrated in these case studies, the optimal allocation of energy storage is driven by the profit maximization condition in Section IV-D.

VI. CONCLUSIONS AND FUTURE WORK

In this study we investigate the interaction between the locational marginal price (LMP) and storage dynamics with a modified IEEE 14-bus benchmark system. To illustrate LMP-based storage dynamics, we extended the OPF formulation with storage dynamics in [13] and [15] to account for roundtrip efficiency of the storage, thermal limits, of lines, and ramp rates for conventional generators. We demonstrate that explicitly accounting for charging and discharging dynamics enables us to model additional properties of the problem, and thus gain greater insight into optimal ESS integration. We then apply a rank relaxation convexify the OPF problem with storage dynamics in order to present the storage subproblem and associated theory on optimal storage

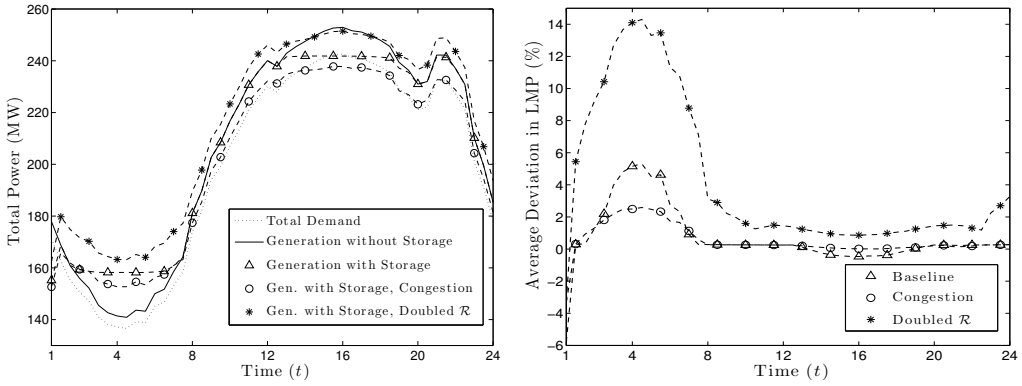

(a) (b)

Fig. 3: (a) Total generation on the power network. (b) The average deviation in LMP for optimizing the SDP-OPF+S problem with no storage compared to optimization with storage, for the given baseline, congestion, and doubled $\mathcal{R}$ scenarios.

dynamics. Our main result proves that storage allocation and operation is driven by the incremental profit that an ESS installation can accrue at a location for a given operating horizon. As a result, maximizing the storage operator's profits is naturally the dual to minimizing the system operator's costs (see Corollary 1 in Section IV-D).

The current work demonstrates the significance of LMPs in driving storage dynamics at low penetrations of ESS integration. Our ongoing work includes quantifying the sensitivities of the LMPs at the optimal solution in order to assess the marginal impact of properties such as line impedance characteristics, thermal line limits, marginal cost of generators, and demand response. We are also extending the analysis to examine how different utility-scale energy storage technologies can be allocated and operated to facilitate increasing integration of renewable energy resources.

ACKNOWLEDGMENTS

This work was partially supported by NSF ECCS 1230788 and OISE 1243482. The authors would like to thank B. F. Hobbs and R.P. O'Neill for many valuable discussions during the course of this work.

REFERENCES

[1] R. Sioshansi, P. Denholm, and T. Jenkin, "Market and policy barriers to deployment of energy storage," *Economics of Energy and Environmental Policy*, vol. 1, no. 2, pp. 47–63, 2012.

[2] P. Denholm et al., "The role of energy storage with renewable electricity generation," National Renewable Energy Laboratory, Tech. Rep. NREL/TP-6A2-47187, 2010.

[3] E. Drury, P. Denholm, and R. Sioshansi, "The value of compressed air energy storage in energy and reserve markets," *Energy*, vol. 36, pp. 4959–4973, 2011.

[4] M. Kintner-Meyer et al. , "National assessment of energy storage for grid balancing and arbitrage: Phase 1, WECC," U.S. Department of Energy, Tech. Rep. DE-AC05-76RL01830, 2012.

[5] R. Sioshansi et al., "Estimating the value of electricity storage in PJM: Arbitrage and some welfare effects," *Energy*, vol. 31, pp. 269–277, 2009.

[6] H. Bludszuweit and J. A. Dominguez-Navarro, "A probabilistic method for energy storage sizing based on wind power forecast uncertainty," *IEEE Trans. on Power Systems*, vol. 26, no. 3, pp. 1651–1658, 2011.

[7] T. K. A. Brekken et al., "Optimal energy storage sizing and control for wind power applications," *IEEE Trans. on Sustainable Energy*, vol. 2, no. 1, pp. 69–77, 2011.

[8] K. M. Chandy et al., "A simple optimal power flow model with energy storage," in *Proc. of the 49th IEEE Conf. on Decision and Control*, 2010, pp. 1051–1057.

[9] K. Dvijotham, S. Backhaus, and M. Chertkov, "Operations-based planning for placement and sizing of energy storage in a grid with a high penetration of renewables," Los Alamos National Lab., Tech. Rep., 2011.

[10] M. Ghofrani et al., "A framework for optimal placement of energy storage units within a power system with high wind penetration," *IEEE Trans. on Sustainable Energy*, vol. 4, no. 2, pp. 434–442, 2013.

[11] E. Benedict et al., "Losses in electric power systems," Purdue University, Tech. Rep., 1992.

[12] Y. M. Atwa and E. F. El-Saadany, "Optimal allocation of ESS in distribution systems with a high penetration of wind energy," *IEEE Trans. on Power Systems*, vol. 25, no. 4, pp. 1815–1822, 2013.

[13] S. Bose et al., "Optimal placement of energy storage in the grid," in *Proc. of the 51st IEEE Conf. on Decision and Control*, 2012, pp. 5605–5612.

[14] A. Gabash and P. Li, "Active-reactive optimal power flow in distribution networks with embedded generation and battery storage," *IEEE Trans. on Power Systems*, vol. 27, no. 4, pp. 2026–2035, 2012.

[15] D. F. Gayme and U. Topcu, "Optimal power flow with large-scale storage integration," *IEEE Trans. on Power Systems*, vol. 28, no. 2, pp. 709–717, 2013.

[16] Z. Hu and W. T. Jewell, "Optimal power flow analysis of energy storage for congestion relief, emissions reduction, and cost savings," in *Proc. of the IEEE PES Systems Conf. and Exposition*, 2011.

[17] R. P. O'Neill, T. Dautel, and E. Krall, "Recent ISO software enhancements and future software and modeling plans," Federal Energy Regulatory Commission, Tech. Rep., 2011.

[18] M. B. Cain, R. P. O'Neill, and A. Castillo, "Optimal power flow papers: Paper 1. history of optimal power flow and formulations," Federal Energy Regulatory Commission, Tech. Rep., 2013.

[19] X. Bai et al., "Semidefinite programming for optimal power flow problems," *Int'l Journal of Electrical Power and Energy Systems*, vol. 30, no. 6-7, pp. 383–392, 2008.

[20] J. Lavaei and S. H. Low, "Zero duality gap in optimal power flow problem," *IEEE Trans. on Power Systems*, vol. 27, no. 1, pp. 92–107, 2012.

[21] U. of Washington, "Power systems test case archive," 1993. [Online]. Available: http://www.ee.washington.edu/research/pstca

[22] R. D. Zimmerman, C. E. Murillo-Snchez, and R. J. Thomas, "Matpower: Steady-state operations, planning and analysis tools for power systems research and education," *IEEE Trans. on Power Systems*, vol. 26, no. 1, pp. 12–19, 2011.